Energy Reception for Mobile Radio

By E. N. GILBERT

(Manuscript received July 2, 1965)

Statistical properties are derived for mathematical models of the multipath fading encountered in mobile radio. These properties are used to compare some receiving systems which use several antennas to combat fading. Particular attention is given to a system of J. R. Pierce which has electric and magnetic dipole antennas and computes the electromagnetic energy density at a point. The statistical properties considered here include energy density distribution functions, correlation coefficients, and the power spectrum of the energy density observed at a moving point.

I. INTRODUCTION

A radio signal may reach a receiver via several paths because of reflections from nearby objects. If the receiver is a mobile radio installation, the received field strength may fluctuate wildly because the reflected waves add with changing relative phases as the receiver moves. J. R. Pierce* has suggested a way to combat these fluctuations by using three antennas.

As background for Pierce's idea consider the standing wave pattern produced when a plane wave is reflected at normal incidence from a large wall. An electric dipole antenna moving toward the wall finds nulls in the electric field repeated at half-wavelength intervals. However, these nulls occur at maxima of the magnetic field. In fact, the total electromagnetic energy density $\frac{1}{2}(\epsilon \mid E \mid^2 + \mu \mid H \mid^2)$ is constant throughout the pattern.

In Pierce's scheme, the transmitter radiates a vertically polarized wave. The receiver carriers a vertical electric dipole antenna and also a pair of loop antennas with axes perpendicular to each other and to the dipole. These three antennas receive the three nonzero field components E_z, H_x, and H_y. The three antenna signals enter separate square-law detectors and the three detector outputs are added to

* Private communication.

obtain $\frac{1}{2}(\epsilon \mid E_z \mid^2 + \mu \mid H_x \mid^2 + \mu \mid H_y \mid^2) = \psi_T$, the total energy density. If the signal is amplitude modulated, the receiver may compute $\psi_T^{\frac{1}{2}}$ in order to achieve linear detection.

The output of this *energy receiver* remains constant as the receiver moves through the above-mentioned standing wave pattern near a wall. In more complicated interference patterns the total energy density does fluctuate, although hopefully not as much as the electric energy density alone. This paper examines some superpositions of vertically polarized plane waves in order to compare the energy receiver with a receiver which observes only the electric field. Two other receivers are examined briefly in Section V. One is a *diversity receiver* which has two or more electric dipole antennas and a switching system to select the antenna with the strongest signal. The second squares and adds the outputs of several electric dipoles.

Most of the analysis in this paper applies slightly more generally to a *weighted energy detector* which combines the electric and magnetic energy densities with weight factors $2d$ and $2b$ to obtain $d\epsilon \mid E \mid^2 + b\mu \mid H \mid^2$ (this is the energy density ψ_T if $d = b = \frac{1}{2}$). Sections III and IV show that certain unequal weights have some slight advantages.

In order to imitate the haphazardness of real mobile radio interference patterns most of the field models which follow assume waves with randomly chosen amplitudes, phases, and directions of propagation. Section IV finds probability distributions for the weighted energy density. At wavelengths longer than about 0.2 meters, such distributions might be used to predict the fraction of time that the signal will fade beyond the range of the receiver's AVC action. At shorter wavelengths, a fast automobile encounters fluctuations which have appreciable components at audible frequencies. Then questions about spectra (Section VIII) and correlations (Section VII) arise.

Fig. 1 shows the energy density as a function of position when four waves superimpose. The four waves had equal amplitudes but the phases and directions were chosen to typify some of the random models which follow. The propagation directions made angles of 0°, 60°, 140°, and 260° which were measured clockwise away from a horizontal direction. Table I gives the code for interpreting the printed symbols as energy densities in db above the mean level. The square in Fig. 1 is 3.6 wavelengths on a side. Fig. 2 uses the same four waves and the code of Table I to depict the electric energy density alone. It is immediately apparent that Fig. 2 represents a more violent function than Fig. 1. The peaks are higher (usually above 4 db), the valleys are deeper (often below −13 db), and intermediate levels are relatively scarce.

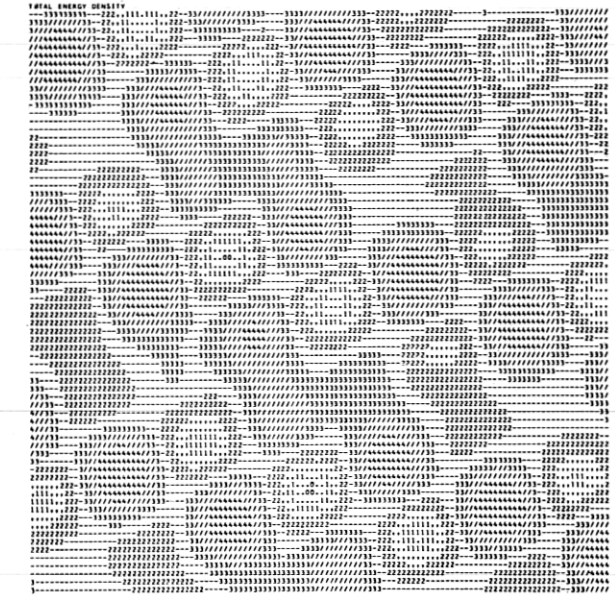

Fig. 1 — Total energy density of four superimposed waves.

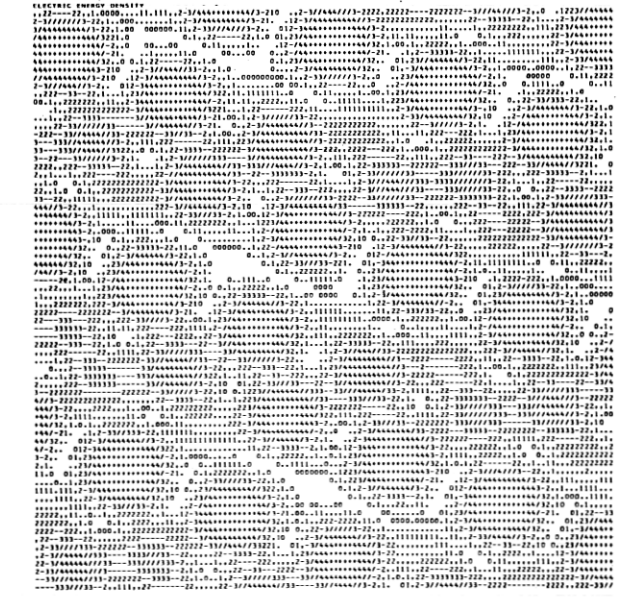

Fig. 2 — Electric energy density of four superimposed waves.

TABLE I — INTERPRETATION OF FIGS. 1 AND 2

Symbol	Interpretation
blank	below −13 db
0	between −13 db and −10 db
.	" −10 " " −7 "
1	" −7 " " −5 "
,	" −5 " " −3 "
2	" −3 " " −1 "
-	" −1 " " 0 "
3	" 0 " " 1 "
/	" 1 " " 2 "
4	" 2 " " 4 "
+	above 4 db

II. NOTATION

Fields will be functions of Cartesian coordinates (x,y) in a horizontal plane. The propagation direction of a vertically polarized wave will be specified by a unit vector $u = (u_x, u_y)$. Let P be the radius vector to a point in the (x,y) plane. At P, the following are the nonzero field components of a wave propagating in direction u:

$$E_z = \epsilon^{-\frac{1}{2}} A \exp\{-i\beta u \cdot P\}$$

$$H_x = \mu^{-\frac{1}{2}} u_y A \exp\{-i\beta u \cdot P\}$$

$$H_y = -\mu^{-\frac{1}{2}} u_x A \exp\{-i\beta u \cdot P\}$$

where $2\pi/\beta$ is the wavelength and A is a complex amplitude. All fields depend on time through a complex factor $\exp i\omega t$ which will be suppressed. The factors containing the dielectric constant ϵ and permeability μ were inserted to simplify the expressions for energy density. When waves from directions $u,v,w, \cdots$ are added, their amplitudes will be called $A(u), A(v), A(w), \cdots$. Most of this paper is concerned with the weighted energy density

$$\begin{aligned} \psi(P) = {} & d \left| \sum_u A(u) \exp - i\beta u \cdot P \right|^2 \\ & + b \left| \sum_u A(u) u_y \exp - i\beta u \cdot P \right|^2 \\ & + b \left| \sum_u A(u) u_x \exp - i\beta u \cdot P \right|^2. \end{aligned} \tag{1}$$

The coefficients d and b in (1) will always be nonnegative and will satisfy $d + b = 1$. Let $\psi_E(P)$ and $\psi_H(P)$ denote the electric and magnetic energy densities at P; then $\psi(P) = 2d\psi_E(P) + 2b\psi_H(P)$. The choice $d = b = \frac{1}{2}$ makes $\psi(P)$ the total energy density $\psi_T(P)$; $\psi(P)$ can also

become $2\psi_E(P)$ or $2\psi_H(P)$ if one adopts the extreme values $d = 1$ or $b = 1$. Another form of (1) is

$$\psi(P) = \sum_{u,v} A(u)A^*(v)(d + bu\cdot v) \exp i\beta(v - u)\cdot P \qquad (2)$$

where * denotes complex conjugate.

The average level ψ_0 about which $\psi(P)$ fluctuates, may be defined as the limit as $R \to \infty$ of the average of $\psi(P)$ over a circle of radius R. In the limit, terms of (2) with $v \neq u$ contribute zero to the average. Thus, if no two propagation directions are the same the average level is

$$\psi_0 = \sum_u |A(u)|^2. \qquad (3)$$

When $d = 1$ or $b = 1$, (3) shows that the average electric and magnetic energy densities are each $\frac{1}{2}\psi_0$.

According to (3), ψ_0 does not depend on d and b. The influence of d and b on some properties of the multipath fluctuations will be examined in subsequent sections, and (3) guarantees that the average detector output remains constant as d and b vary. When making such comparisons it must be recognized that the random noise received by the system may depend on d and b. For example, if the three antennas receive uncorrelated noises of equal power the noise output of the detector is proportional to $d + 2b$.

III. NULLS

Since three complex equations $E_z = 0$, $H_x = 0$, $H_y = 0$ must hold simultaneously at a point of zero energy density, it is not obvious when such a zero is possible. This section gives some examples of zeros.

When fewer than four waves add, no two having the same direction of propagation, no point can be a point of zero energy density. A proof of this fact is given in Appendix A. However, it is not necessarily desirable to have only a small number of waves. For example, consider two waves propagating in directions which differ by an angle ϑ, say $u = (\cos\frac{1}{2}\vartheta, \sin\frac{1}{2}\vartheta)$ and $v = (\cos\frac{1}{2}\vartheta, -\sin\frac{1}{2}\vartheta)$. Suppose the amplitudes are equal in magnitude but differ in phase by δ, say

$$A(u) = \exp(i(\varphi + \delta)), \qquad A(v) = \exp(i\varphi).$$

At a point $P = (x, y)$, (1) and (3) show that

$$\psi(P) = \psi_0\{1 + (d + b\cos\vartheta)\cos(\delta - 2\beta y \sin\tfrac{1}{2}\vartheta)\}. \qquad (4)$$

Note that $\psi(P)$ attains its minimum value $\psi_0\{1 - |d + b\cos\vartheta|\}$

along the family of lines

$$(2\beta \sin \tfrac{1}{2}\vartheta)y = \delta + \text{multiple of } \pi. \tag{5}$$

The "multiple" in (5) must be odd if $d + b \cos \vartheta > 0$ and even if $d + b \cos \vartheta < 0$. The (positive) minimum value can be arbitrarily small if ϑ is small enough.

It is interesting to compare the weighted energy density (4) with the electric energy density $\psi_E(P)$. When $d = 1$, (4) becomes

$$\psi_E(P) = \tfrac{1}{2}\psi_0\{1 + \cos(\delta - 2\beta y \sin \tfrac{1}{2}\vartheta)\} \tag{6}$$

a function which vanishes along the lines (5).

Equation (4) may be used to help decide a good choice of the coefficients d,b for a detector. Imagine the two waves produced at random in such a way that the angle ϑ and relative phase δ are independent random variables, both having probability density $(2\pi)^{-1}$ in the interval $(0, 2\pi)$. One wants $\psi(P)$ to fluctuate as little as possible. The variance of the random variable $\psi(P)$ is one measure of fluctuation. From (4) one obtains a variance

$$E\{|\psi(P) - \psi_0|^2\} = \tfrac{1}{2}\psi_0^2\{d^2 + \tfrac{1}{2}b^2\}$$

which has its minimum when $d = \frac{1}{3}$, $b = \frac{2}{3}$. Alternatively, one might prefer to pick d and b so that the expectation of the minimum value $1 - |d + b \cos \vartheta|$ of $\psi(P)$ is as large as possible. This condition requires d and b to minimize $E\{|d + b \cos \vartheta|\}$. The calculation given in Appendix B shows that the minimizing d and b are $d = 0.40$, $b = 0.60$. Although both criteria suggest that the magnetic energy density be weighted more than the electric energy density, both minima are so broad that an energy detector with $d = b = \frac{1}{2}$ does almost as well.

It is possible to have $\psi(0) = 0$ when waves from four different directions superimpose. For example, take the propagation directions along the $\pm x$, $\pm y$ coordinate axes

$$u = (1,0), \qquad v = (0,1), \qquad -u = (-1,0), \qquad -v = (0,-1)$$

and let the amplitudes be

$$A(u) = A(-u) = 1, \qquad A(v) = A(-v) = -1.$$

At the point $P = (x, y)$,

$$\psi(P) = \psi_0\{d(\cos \beta x - \cos \beta y)^2 + b(\sin^2 \beta x + \sin^2 \beta y)\}.$$

Zeros are spaced $\lambda/\sqrt{2}$ apart in this pattern if $b \neq 0$. However the

electric density is much worse,

$$\psi_E(P) = \tfrac{1}{2}\psi_0\{\cos \beta x - \cos \beta y\}^2.$$

The zeros of $\psi_E(P)$ are not isolated, they occupy two orthogonal families of parallel lines.

IV. ENERGY DISTRIBUTION FUNCTIONS

Three real parameters specify a wave, say the angle ϑ between u and the x axis, and the modulus $| A(u) |$ and phase of the complex amplitude $A(u)$. This section discusses some models which pick at random the $3N$ parameters of N interfering waves. In every case the N phases are chosen independently with constant probability density $(2\pi)^{-1}$ in the range $(0,2\pi)$. As a result, the models are stationary with respect to translations of the (x,y) coordinate system. In particular the probability distribution function of $\psi(P)$ is the same for all points P; to simplify the analysis take $P = 0$, the origin. The distribution function

$$F(\psi) = \text{Prob}\{\psi(0) \leqq \psi\}$$

is the probability that the detector of a mobile radio station produces an output less than ψ. In this section, the N waves have roughly the same statistical properties. By contrast Section VI considers a model in which one of the waves represents a strong wave direct from the transmitter.

In the first model the number of waves is $N \geqq 3$. The N propagation vectors $u_1, \cdots, u_N$ are not random. They are equally spaced around the unit circle; u_k makes angle $2\pi k/N$ with the positive x-axis. Each complex amplitude $A(u)$ will have the form $A(u) = R(u) + iI(u)$ where the $2N$ real numbers $R(u_1), \cdots, R(u_N), I(u_1), \cdots, I(u_N)$ are supposed independent Gaussian random numbers with mean 0 and variance 1. Another way to obtain the same random process is to pick moduli $| A(u_1) |, \cdots, | A(u_N) |$ independently from a Rayleigh distribution and the N phases independently with constant density $(2\pi)^{-1}$ in the range 0 to 2π.

According to (3), the average of $\psi(P)$ over the plane is

$$\psi_0 = \sum_u R^2(u) + \sum_u I^2(u)$$

so that the expected average is

$$\bar{\psi} = E(\psi_0) = 2N. \tag{7}$$

Appendix C derives the distribution function

$$F(\psi) = 1 - c^2 \exp(-\psi'/d) + (c-1)\{c + 1 + 2\psi'/d\} \exp(-2\psi'/b) \tag{8}$$

where $c = 2d/(2d - b)$ and $\psi' = \psi/\bar{\psi}$. Note that the number of waves N enters (8) only through the normalizing factor $\bar{\psi} = 2N$. The distribution function for the total energy is (8) with $c = 2$. From the limiting cases $d = 1$ and $d = 0$ of (8) one obtains distribution functions for the electric and magnetic energy densities.

$$\text{Prob}\{\psi_E(0) \leqq (\tfrac{1}{2}\bar{\psi})\psi'\} = 1 - \exp(-\psi')$$

$$\text{Prob}\{\psi_H(0) \leqq (\tfrac{1}{2}\bar{\psi})\psi'\} = 1 - (1 + 2\psi')\exp(-2\psi').$$

Curves EN and TN in Fig. 3 show the distributions of electric and total energy densities plotted in db above their respective mean average levels. The electric energy density has a much higher probability of being small than the total energy density. A curve for the magnetic energy density will be given in Section V.

The distribution obtained for $\psi_E(0)$ implies that the electric field strength $|E_z|$ has a Rayleigh distribution. In this respect, the model agrees with some experimental data of W. R. Young[5] (see in particular his Fig. 5).

For small values of ψ, (8) becomes

$$F(\psi) = (\tfrac{2}{3})d^{-1}b^{-2}\psi'^3 + \cdots$$

with missing terms $\cdots$ of order $0(\psi'^4)$ (see (24)). To make small values of ψ as unlikely as possible, one may minimize $d^{-1}b^{-2}$ by picking $d = \frac{1}{3}$, $b = \frac{2}{3}$. Recall that these values had another minimizing property in Section III. Again the advantage over using $d = b = \frac{1}{2}$ is slight. If the curve for $d = \frac{1}{3}$, $b = \frac{2}{3}$ were plotted in Fig. 3 it would lie about $\frac{1}{4}$ db to the right of the total energy density distribution curve. Equation (8) becomes indeterminate when $d = \frac{1}{3}$, $b = \frac{2}{3}$. However, in this special case, $\psi(0)$ has a chi-squared distribution of six degrees of freedom

$$F(\psi) = 1 - (1 + 3\psi' + \tfrac{1}{2}(3\psi')^2)\exp - 3\psi'.$$

Part of the variability of $\psi(0)$ comes from the randomness of the average value ψ_0. For any particular choice of the wave amplitudes, ψ_0 will not be exactly $\bar{\psi}$; the distribution of $\psi(0)/\psi_0$ might have been more relevant. However, ψ_0 has a chi-squared distribution with $2N$ degrees of freedom and so has high probability of being close to $\bar{\psi}$, say within 0.5 db, especially when N is large.

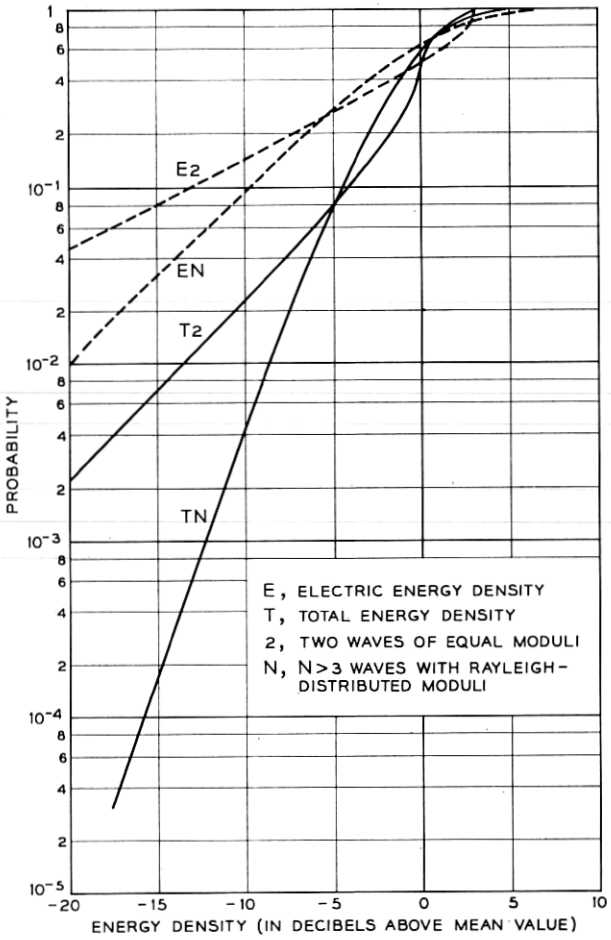

Fig. 3 — Probability distribution functions for energy densities.

The simple form of the distribution (8) results from the special random process which picks the amplitudes and directions. One might prefer to choose directions independently at random with probability $\vartheta/2\pi$ of making an angle less than ϑ with the x-axis. Other amplitude distributions also suggest themselves. It seems reasonable to continue to insist on independent amplitudes with random phases but one might use equal moduli $| A(u) |$ or another modulus distribution instead of the Rayleigh distribution. Undoubtedly $F(\psi)$ will be a more complicated function of N in these cases. However, (8) must still apply in the limit

of large N. For example, let M be an integer approximately equal to $N^{\frac{1}{2}}$. Let $v_1, \cdots, v_M$ be M unit vectors equally spaced around the unit circle. For each wave direction u find the vector u' in the list $v_1, v_2, \cdots, v_M$ which approximates u as closely as possible (and so to within angle π/M). If N is large, one makes only a small error in $\psi(0)$ by replacing each true direction u in (1) by its approximation u'. This approximation replaces the waves with random directions by waves with M equally spaced directions. For $i = 1, \cdots, M$ the approximating waves with direction v_i add up to a single wave, say with amplitude $A'(v_i)$. The central limit theorem shows that the real and imaginary parts of $A'(v_i)$ have approximately Gaussian distributions when N is large. Then the assumptions leading to (8) hold again.

Limiting results may be misleading if applied when the number of waves is small, as may be typical in mobile radio. Curves $T2$ and $E2$ of Fig. 3 show distributions for the total energy density and electric energy density (plotted in db above their mean values) for a superposition of two waves with equal moduli, random phases, and random directions. The distribution of total energy density $\psi_T(0)$ was obtained numerically using (4) with $d = b = \frac{1}{2}$; $\psi_T(0)$ was evaluated for 200 equally spaced values of ϑ and 200 equally spaced values of δ. A histogram of the 40,000 numbers was compiled to get the distribution. The electric energy distribution is easily derived from (6):

$$\text{Prob}\,\{\psi_E(0) \leqq (\tfrac{1}{2}\psi_0)\psi'\} = \pi^{-1} \arccos\,(1 - \psi')$$

(see Margaret Slack[4] for the electric energy distribution when other numbers of random waves of equal moduli combine). The curves show that the case of two waves of equal moduli is much worse for mobile radio than the case of waves with Rayleigh distributed moduli. Nevertheless total energy detection is again much better than electric energy detection.

When more than two waves of equal moduli, random phases, and random directions combine, the total energy density $\psi_T(0)$ depends on many random parameters. To find its distribution function by a numerical integration of the kind used for two waves would be much too costly. A computer experiment was used instead. Using pseudo-random numbers to pick phases and directions, the computer generated a sequence of field components for independent plane waves. After computing each new wave the computer found for $N = 2, \cdots, 10$, the energy density in the sum of the N most recently computed waves. After 10,009 waves, the computer had compiled histograms of the energy

densities in sums of 2, 3, $\cdots$, 10 waves, each based on 10,000 random samples. The same wave appeared in N consecutive sums of N waves; then samples closer together than N were not independent. However, the estimate of $F(\psi)$ is at least as good as if the experiment had $10{,}000/N$ independent samples.

Table II summarizes this experiment and compares the observations with theoretical predictions based on the curves in Fig. 3. The numbers observed agree surprisingly well with (8) even when $N = 3$. A comparison of the theoretical and observed numbers for $N = 2$ gives an idea of the accuracy of the experiment.

V. RECEPTION USING M ELECTRIC DIPOLES

Let m vertical dipole antennas be placed at points $P_1, \cdots, P_m$. Using switched diversity reception the received signal energy density is

$$\psi_D = \max \{\psi_E(P_1), \cdots, \psi_E(P_m)\}.$$

Another possibility is to square the antenna signals and add them (additive diversity); then the detector output is

$$\psi_S = \psi_E(P_1) + \psi_E(P_2) + \cdots + \psi_E(P_m).$$

$P_1, \cdots, P_m$ will be assumed spaced so far apart that the fields at these points may be considered independent random variables. If there are N waves generated at random by the first model of Section III, then each term $\psi_E(P_i)$ is a random variable with the chi-squared distribution of two degrees of freedom and mean N.

TABLE II — FRACTION OF SUMS OF N WAVES OF ENERGY DENSITY $\leqq \psi$. SAMPLE SIZE IS 10,000

ψ/ψ_0 in db	$N = 2$ theor	$N = 2$ obs	$N = 3$ obs	$N = 5$ obs	$N = 10$ obs	large N Eq. (8)
−16	0.0057	0.0066	0.0002	0	0	0.00008
−14	0.0091	0.0084	0.0002	0.0003	0	0.0003
−12	0.0144	0.014	0.0004	0.0003	0.001	0.0011
−10	0.0232	0.025	0.0004	0.002	0.003	0.0042
−8	0.0376	0.038	0.006	0.009	0.010	0.0144
−6	0.0614	0.063	0.030	0.033	0.047	0.0459
−4	0.1037	0.104	0.105	0.120	0.117	0.1301
−2	0.1851	0.185	0.227	0.270	0.296	0.3103
0	0.5000	0.500	0.530	0.574	0.584	0.5869
2	0.8908	0.891	0.882	0.853	0.849	0.8484
4	1	1	0.995	0.989	0.979	0.9742
6	1	1	1	1	1	0.9986

The distribution function for ψ_D is

$$F_D(\psi) = \text{Prob } (\psi_D \leqq \psi) = \prod \text{Prob } \{\psi_E(P_i) \leqq \psi\}$$
$$= \{1 - \exp (-\psi/N)\}^m.$$

The mean of ψ_D is

$$\bar{\psi}_D = \int_0^\infty \{1 - F_D(\psi)\} d\psi = \sum_{k=1}^{m} \binom{m}{k} (-1)^{k+1}/k.$$

For $m = 1, 2, \cdots, 5$, $\bar{\psi}_D$ is N, $3N/2$, $11N/6$, $25N/12$, $137N/60$. Then

$$F_D(\psi) = \{1 - \exp (-3\psi/2\bar{\psi}_D)\}^2 \qquad \text{when } m = 2$$
$$F_D(\psi) = \{1 - \exp (-11\psi/6\bar{\psi}_D)\}^3 \qquad \text{when } m = 3, \text{ etc.}$$

ψ_S has the chi-squared distribution with $2m$ degrees of freedom and mean Nm. Fig. 4 shows the distribution function of ψ_S with $m = 2$, 3, 5, and 8. The curves for the distributions of ψ_D and ψ_S lie very close and so the curves for ψ_D were not added to Fig. 4.

When $m = 3$ the distribution function of ψ_S is exactly the same as the one for the weighted energy density $\psi(0)$ with $d = \frac{1}{3}$ and $b = \frac{2}{3}$. As noted in Section IV, this distribution function is slightly better than the one for the energy density ($d = b = \frac{1}{2}$) at small values of ψ.

In Section IV, the two magnetic field components $H_x(0)$ and H_y were found to be uncorrelated. Then the distribution function of the magnetic energy density at zero follows the curve labeled $m = 2$ in Fig. 4.

VI. STRONG DIRECT WAVE

Section IV presented extreme cases in which the waves are all roughly of comparable strength. In this section another wave, stronger than the others, will be added to represent a "direct" wave of amplitude R. It is no longer easy to derive $F(\psi)$ exactly. However, the asymptotic form of $F(\psi)$ for small values of ψ is derived in Appendix C using the first model of Section IV. This result (25) assumes a convenient form in terms of the quantity

$$\sigma = 2N/\bar{\psi} = 1 - R^2/\bar{\psi}$$

which represents the fraction of the expected weighted energy density $\bar{\psi}$ contributed by the N scattered waves. When N and R are expressed in terms of $\bar{\psi}$ and σ the final result is

$$F(\psi) = (\tfrac{2}{3}) d^{-1} b^{-2} \sigma^{-3} (\psi/\bar{\psi})^3 \exp - 3(\sigma^{-1} - 1) \qquad (9)$$

approximately for small ψ.

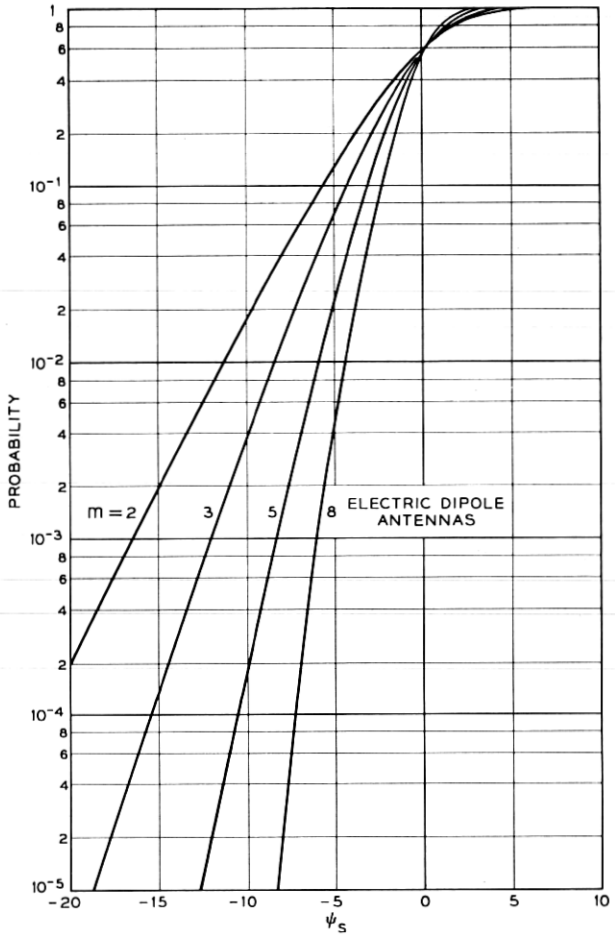

Fig. 4 — Probability distribution function for the sum ψ_s of the electric energy densities at m points.

The case $R = 0$, or $\sigma = 1$, was discussed in Section IV. When $0 < \sigma < 1$, (9) contains the extra factor

$$\sigma^{-3} \exp - 3(\sigma^{-1} - 1)$$

which is less than 1 and approaches 0 with decreasing σ. One concludes that $F(\psi)$ is then smaller than the value given by (8); i.e., deep minima tend to be less frequent when a direct wave is present. For example, if scattered waves account for only half the received weighted energy density ($\sigma = \frac{1}{2}$), the probability of receiving less weighted energy

density than ψ is only 8 exp $-$ 3 = 0.40 times the probability (8) for $\sigma = 1$.

VII. CORRELATION COEFFICIENTS

This section finds correlation coefficients between various pairs of energy densities. The correlation coefficient between $\psi(0)$ and $\psi(P)$ indicates whether a receiver traveling from 0 to P will find very different weighted energy densities at the two points. The correlation coefficient between $\psi_E(0)$ and $\psi_E(P)$ might be used to decide whether 0 and P are good locations for two electric dipole antennas in a diversity system; one would want low or negative correlation. For similar reasons, correlation coefficients involving the magnetic energy density $\psi_H(P) = \psi(P) - \psi_E(P)$ are interesting.

The waves in this section are produced by a random process slightly more general than the one used to get Table I. The N propagation directions and N phases are chosen at random and independently as in Section IV. The moduli $| A(u_1(| , \cdots , | A(u_N) |$ are now chosen independently from a common probability distribution. It is not necessary to know the distribution in detail. Only the expected values of the second and fourth powers $E(| A |^2)$, $E(| A |^4)$ enter into the correlation coefficients. To facilitate comparisons with Section IV, take $E(| A |^2) = 2$. Then the expected average weighted energy density is again

$$\bar{\psi} = 2N.$$

R. H. Clarke has also used this random process in an unpublished study of some different correlations.

It will be convenient to express the fourth power moment as

$$E(| A |^4) = 4 + \Sigma^2,$$

so that Σ^2 is the common variance of the squared moduli. When the moduli are all the same, $| A(u_i) | = 2^{\frac{1}{2}}$, $i = 1, \cdots , N$, and the variance Σ^2 is zero. When moduli have the Rayleigh distribution, $\Sigma^2 = 4$.

All the correlation coefficients of interest will be obtained as special cases of a single result. Consider two weighted energy densities.

$$\psi_1 = 2d\psi_E(0) + 2b\psi_H(0)$$

and

$$\psi_2 = 2D\psi_E(P) + 2B\psi_H(P).$$

Appendix D proves

$$E(\psi_1\psi_2) - E(\psi_1)E(\psi_2) = N\Sigma^2 + 4N(N-1)\{dDJ_0^2(\beta r) + (dB + bD)J_1^2(\beta r) + \tfrac{1}{2}bB(J_0^2(\beta r) + J_2^2(\beta r))\} \quad (10)$$

where $r = |P|$. When $D = d$, $B = b$, and $P = 0$, then $\psi_2 = \psi_1$ and (10) becomes the variance of ψ_1

$$\text{Var } \psi_1 = N\Sigma^2 + (4d^2 + 2b^2)N(N-1). \quad (11)$$

Likewise,

$$\text{Var } \psi_2 = N\Sigma^2 + (4D^2 + 2B^2)N(N-1). \quad (12)$$

The coefficient of correlation between ψ_1 and ψ_2 is

$$\rho = \{E(\psi_1\psi_2) - E(\psi_1)E(\psi_2)\} / \{\text{Var } \psi_1 \text{ Var } \psi_2\}^{\frac{1}{2}}, \quad (13)$$

which may be evaluated using (10), (11), and (12). The case of equal moduli ($\Sigma^2 = 0$) is especially simple because then (assuming $N > 1$) the factors $N(N-1)$ cancel out and ρ does not depend on N. This is the only case in which $\rho \to 0$ as $r \to \infty$; when $\Sigma^2 > 0$ the average weighted energy density ψ_0 is uncertain and so the energy densities remain slightly correlated even at points far apart. When N is large this residual correlation is small and ρ approaches its value for equal moduli.

By choosing special values for d, b, D, and B, one can obtain correlation coefficients of special interest:

$$\rho_{TT} = \{3J_0^2(\beta r) + 4J_1^2(\beta r) + J_2^2(\beta r)\}/3$$

$$\rho_{EE} = J_0^2(\beta r)$$

$$\rho_{HH} = J_0^2(\beta r) + J_2^2(\beta r)$$

$$\rho_{ET} = (\tfrac{2}{3})^{\frac{1}{2}}\{J_0^2(\beta r) + J_1^2(\beta r)\}$$

$$\rho_{EH} = 2^{\frac{1}{2}}J_1^2(\beta r)$$

$$\rho_{HT} = 3^{-\frac{1}{2}}\{J_0^2(\beta r) + 2J_1^2(\beta r) + J_2^2(\beta r)\}.$$

Here the subscripts E,H,T indicate the kind of energy, electric, magnetic, or total, at the two points. For the sake of simplicity the coefficients have been given only in the special case of equal moduli ($\Sigma^2 = 0$) or in the limit of large N. Some of the more interesting coefficients are plotted in Fig. 5.

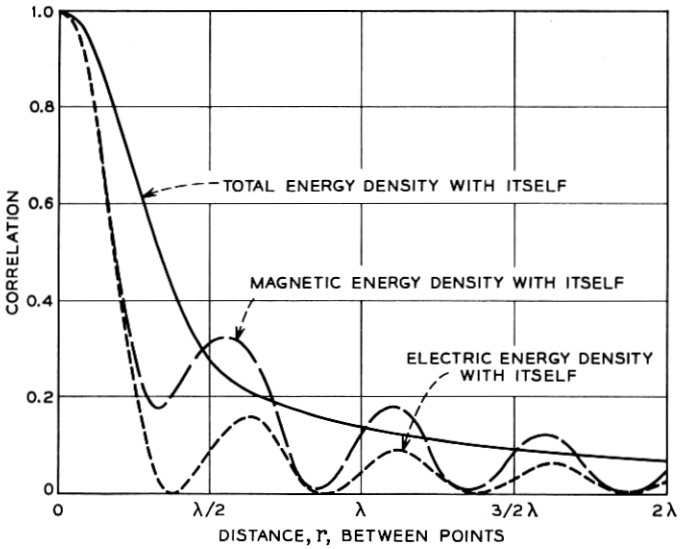

Fig. 5 — Coefficient of correlation between the energy densities at two points separated by distance r.

VIII. SPECTRA

When a receiver moves with constant velocity vector V_0 the received energy density $\psi(V_0t)$ is a random function of time. If one assumes the model of Section VII, the autocorrelation function of $\psi(V_0t)$ is known and hence its power spectrum may be found. The power spectrum of $\psi(V_0t)$ gives some idea of the frequencies at which the fluctuation noise is likely to be strong. In particular cases, depending on the way that the modulating signal is to be extracted from $\psi(P)$, the spectra of other functions may be more important. For example, if an AM system is used, one might prefer to know the power spectrum of $\psi^{\frac{1}{2}}(V_0t)$. For another kind of fading spectrum see J. F. Ossanna[3]. Ossanna combines two random waves and derives the spectrum obtained at the output of an envelope detector receiving the electric field.

For purposes of comparing power spectra it is convenient to normalize them to make the total power unity. Appendix E takes the Fourier transform of $E\{\psi(0)\psi(V_0t)\}/E\{\psi^2(0)\}$ to obtain a normalized spectrum. In order to keep formulas simple, Appendix E and this section consider only the case of large N.

The normalized power spectrum of $\psi(V_0t)$ contains a spectral line at zero frequency which represents the carrier or desired signal. The power

in this line is $1/(1 + d^2 + \frac{1}{2}b^2)$. Again the choice $d = \frac{1}{3}$, $b = \frac{2}{3}$ maximizes this power. The rest of the spectrum is fluctuation noise distributed with a spectral density function $s(f)$. Fig. 6 shows this spectrum for the total energy density and for the electric energy density. Both spectra vanish when f is larger than a cutoff frequency

$$f_0 = 2 \mid V_0 \mid /\lambda. \tag{14}$$

Note that f_0 is the frequency of the fluctuations in electric energy density observed by a vehicle moving toward the wall in the interference pattern described in Section I. When $0 < f \leqq f_0$, the spectral density has an analytic expression (32) in terms of the complete elliptic integrals $K(x)$ and $E(x)$. Let $\nu = f/f_0$. Then

$$s(f) = \frac{16}{33\pi^2 f_0} \{(3 - \nu^2)K((1 - \nu^2)^{\frac{1}{2}}) - 2(2 - \nu^2)E((1 - \nu^2)^{\frac{1}{2}})\} \tag{15}$$

for the total energy density and

$$s(f) = K\{(1 - \nu^2)^{\frac{1}{2}}\}/(\pi^2 f_0) \tag{16}$$

for the electric energy density.

The fluctuation noise $\psi_T(V_0 t)$ appears to be less troublesome than $\psi_E(V_0 t)$ both because it contains less total power away from the carrier

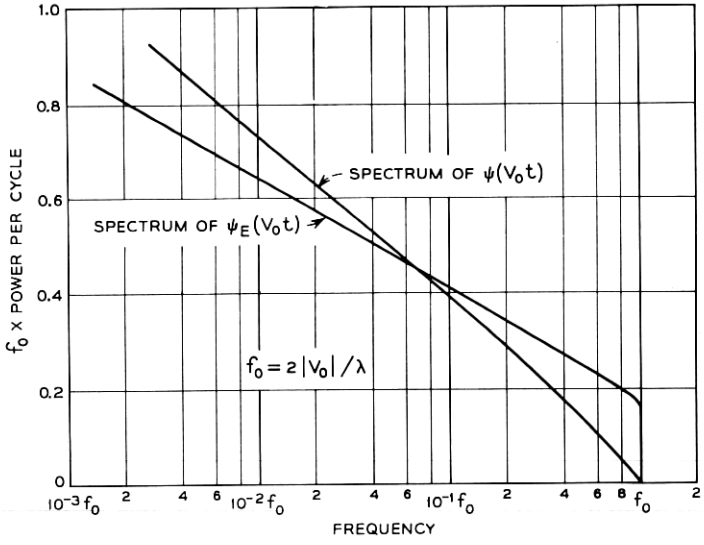

Fig. 6 — Power spectra of the energy densities $\psi(V_0 t)$ and $\psi_E(V_0 t)$ observed by a vehicle moving with constant velocity V_0.

and also because its spectrum is concentrated more toward low frequencies. As Fig. 6 shows, the spectrum of $\psi_T(V_0t)$ goes to 0 smoothly at $f = f_0$ while the spectrum of $\psi_E(V_0t)$ remains at a high level until it drops to 0 discontinuously at $f = f_0$.

IX. ACKNOWLEDGMENTS

I am grateful to J. R. Pierce, who first suggested this problem, R. H. Clarke, C. C. Cutler, and W. C. Jakes, Jr., for much helpful advice and orientation on the subject of mobile radio.

APPENDIX A

The impossibility of producing a zero by adding fewer than four waves

In what follows, waves must have nonzero amplitude and no two waves may have the same propagation direction. It is clearly possible for two or three waves with same direction to cancel if their amplitudes add up to zero.

The condition for a zero at the origin ($P = 0$) is

$$0 = \psi(0) = \left|\sum_u A(u)\right|^2 + \left|\sum_u A(u)u_y\right|^2 + \left|\sum_u A(u)u_x\right|^2$$

or simply

$$0 = \sum_u A(u) = \sum_u A(u)u. \tag{17}$$

Consider first the case of two waves in different directions u and v. Then, (17) becomes

$$A(u) + A(v) = 0.$$

$$A(u)u + A(v)v = 0.$$

The second (vector) equation requires that the unit vectors u,v be colinear. Since v cannot equal u, $v = -u$. Then

$$A(u) + A(v) = 0$$

$$A(u) - A(v) = 0,$$

a system with no solution except the trivial one $A(u) = A(v) = 0$.

When there are three waves with directions u,v,w, one may eliminate $A(w)$ from the system (17) to get

$$A(u)(u - w) + A(v)(v - w) = 0.$$

$A(u)$ cannot be zero. Then

$$u = w + a(v - w)$$

where $a = -A(v)/A(u)$. Since $|u|^2 = |w|^2 = 1$, one finds

$$0 = 2aw \cdot (v - w) + a^2 |v - w|^2. \tag{18}$$

Also,

$$0 = 2w \cdot (v - w) + |v - w|^2 \tag{19}$$

follows similarly from $v = w + (v - w)$ and $|v|^2 = |w|^2 = 1$. Use (19) eliminate $2w \cdot (v - w)$ from (18) and get

$$|v - w|^2 a(a - 1) = 0.$$

Since $v \neq w$ and since $a \neq 0$ (otherwise $A(v) = 0$), $a = 1$. However, if $a = 1$, $u = w + 1(v - w) = v$, a contradiction.

APPENDIX B

Weights which maximize the expected minimum value of $\psi(P)$

In the interference pattern (4) for two random waves, $\psi(P)$ attains a minimum value

$$\psi_{\min} = \psi_0\{1 - |d + b \cos \vartheta|\}.$$

The expected value of $\psi_{\min}$ is

$$E(\psi_{\min}) = \psi_0 \left\{1 - (2\pi)^{-1} \int_0^{2\pi} |d + b \cos \vartheta| \, d\vartheta\right\}. \tag{20}$$

The evaluation of the integral in (20) requires two cases. First, if $b \leqq \frac{1}{2} \leqq d$, $|d + b \cos \vartheta| = d + b \cos \vartheta$ and

$$E(\psi_{\min}) = \psi_0 b, \qquad (b \leqq d). \tag{21}$$

Second, if $d \leqq \frac{1}{2} \leqq b$, let $\vartheta_0 = \cos^{-1}(d/b)$. Then

$$|d + b \cos \vartheta| = \begin{cases} d + b \cos \vartheta & \text{when } |\vartheta \leqq \pi - \vartheta_0 \\ -d - b \cos \vartheta & \text{otherwise} \end{cases}$$

and

$$E(\psi_{\min}) = \psi_0\{b + (2/\pi)(d\vartheta_0 - \sqrt{b^2 - d^2})\}, \qquad (d \leqq b). \tag{22}$$

Fig. 7 shows $E(\psi_{\min})$ plotted vs d. There is a broad maximum near $d = 0.4$, $b = 0.6$.

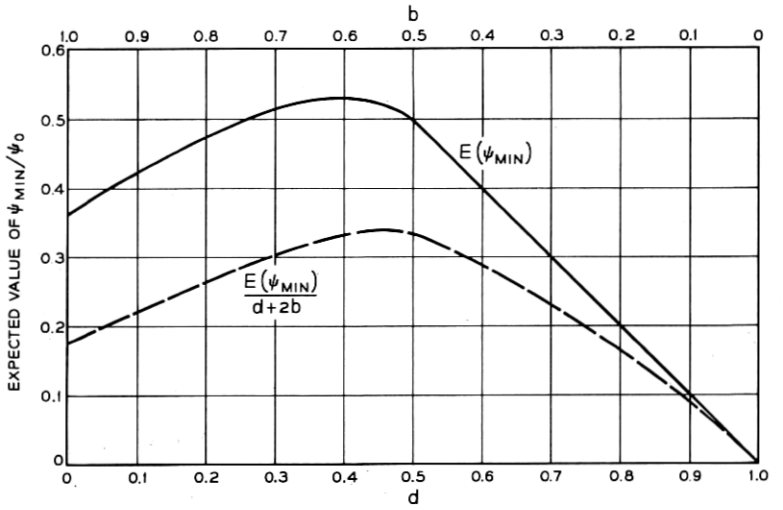

Fig. 7 — $E(\psi_{min})$ and $E(\psi_{min})/(d + 2b)$.

As mentioned in Section II, the received noise power will depend on d and b. One might prefer to maximize the expected minimum signal-to-noise ratio. If the three antennas have uncorrelated noises of equal powers one would then maximize $E(\psi_{\min})/(d + 2b)$. The dashed curve in Fig. 7 shows that $d = 0.45$, $b = 0.55$ for the maximizing detector.

APPENDIX C

The energy distributions (8) and (9)

It is convenient to have a special notation for real and imaginary parts of the field components at $P = 0$. S will always be a real part, J will always be an imaginary part. Subscripts 1, 2, or 3 on S or J denote the field, either $\varepsilon^{\frac{1}{2}} E_z$, $\mu^{\frac{1}{2}} H_x$, or $\mu^{\frac{1}{2}} H_y$. For example, the imaginary part of $\mu^{\frac{1}{2}} H_x$ is

$$J_2 = \sum_u u_y I(u).$$

Each of the six components S_1, J_1, S_2, J_2, S_3, J_3 is a linear combination of the $2N$ Gaussian variables $R(u_1), \cdots, I(u_N)$. Then these six variables have a joint Gaussian distribution, which is determined entirely by its 21-second moments.

All second moments of the form $E(S_i J_j)$ are zero. This follows because $E(R(u)U(v)) = E(R(u))E(I(v)) = 0$ for all N^2 choices of

u,v. Two other typical second moments are:

$$\begin{aligned} E(S_1S_3) &= E\{-\sum_{u,v} R(u)R(v)v_x\} \\ &= -\sum u_x E(R^2(u)) \\ &= -\sum u_x \\ &= -\sum \cos(2\pi k/N), \end{aligned}$$

and

$$\begin{aligned} E(S_2S_3) &= E\{-\sum_{u,v} R(u)R(v)u_y v_x\} \\ &= -\sum_u u_y u_x \\ &= -\tfrac{1}{2}\sum_{k=1}^{N} \sin(4\pi k/N). \end{aligned}$$

The identity

$$\sum_1^N \exp(ikt) = e^{it}\frac{1-\exp(iNt)}{1-\exp(it)}$$

can be used to prove that both are zero. In the first case set $t = 2\pi/N$ and take the real part (recall that $N \geqq 3$ is assumed). In the second case take $t = 4\pi/N$ and take the imaginary part. In like manner, one eventually finds that the only nonzero moments are

$$E(S_1^2) = E(J_1^2) = \sum_u 1 = N$$

$$E(S_2^2) = E(J_2^2) = \sum \sin^2\frac{2\pi k}{N} = \sum\left(\frac{1}{2} - \frac{1}{2}\cos\frac{4\pi k}{N}\right) = \tfrac{1}{2}N$$

$$E(S_3^2) = E(J_3^2) = \sum \cos^2\frac{2\pi k}{N} = \sum\left(\frac{1}{2} + \frac{1}{2}\cos\frac{4\pi k}{N}\right) = \tfrac{1}{2}N.$$

Note that these formulas hold only because $N \geqq 3$. The cases $N = 1$ and 2 are different, having $E(S_2^2) = E(J_2^2) = 0$ and $E(S_3^2) = E(J_3^2) = N$.

The six parts of the field components are independent Gaussian variables with joint probability density function

$$\tfrac{1}{2}(N\pi)^{-3}\exp(-\{S_1^2 + J_1^2 + 2(S_2^2 + J_2^2 + S_3^2 + J_3^2)\}/2N). \quad (23)$$

Now note $\psi(0) = dt_1 + bt_2$ where $t_1 = S_1^2 + J_1^2$ and $t_2 = S_2^2 + J_2^2 + S_3^2 + J_3^2$ are two independent variables with chi-squared distributions.

Then the desired distribution function is

$$F(\psi) = \text{Prob } (dt_1 + bt_2 \leqq \psi)$$
$$= \tfrac{1}{2}N^{-3}\int_0^{\psi/b} t_2 \exp\,(-t_2/N)\int_0^{(\psi-bt_2)/d} \exp\,(-t_1/2N)dt_1dt_2\,.$$

An elementary integration produces the final result (8).

The asymptotic form of $F(\psi)$ for small ψ can be obtained by differentiating (8) or, more simply, by the following argument. According to (23) the joint probability density of $S_1, J_1, S_2, J_2, S_3, J_3$ at the origin is $\frac{1}{2}(N\pi)^{-3}$. The inequality $\psi(0) \leqq \psi$ defines a small ellipsoid

$$d(S_1^2 + J_1^2) + b(S_2^2 + J_2^2 + S_3^2 + J_3^2) \leqq \psi$$

about the origin. This ellipsoid has six-dimensional volume

$$(\pi^3/6)d^{-1}b^{-2}\psi^3.$$

The probability that $(S_1, J_1, \cdots, J_3)$ lies in this ellipsoid is, apart from terms of higher order,

$$F(\psi) = \tfrac{1}{2}(N\pi)^{-3}(\pi^3/6)d^{-1}b^{-2}\psi^3$$
$$F(\psi) = (\tfrac{2}{3})d^{-1}b^{-2}(\psi/\bar{\psi})^3. \tag{24}$$

In Section VI, an additional wave, stronger than the others, was added to represent a "direct" wave. Let the direction u_0 of the direct wave be along the x-axis and let its amplitude be $A(u_0) = R$, a given real number. With $S_1, S_2, \cdots, J_3$ defined again to include the random fields only, the weighted energy density is

$$\psi(0) = d\{(R + S_1)^2 + J_1^2\} + b\{S_2^2 + J_2^2 + (R + S_3)^2 + J_3^2\}$$

with mean $\bar{\psi} = R^2 + 2N$. The asymptotic form of the distribution function for $\psi(0)$ may be derived in the same way as (24). Now the six-dimensional ellipsoid $\psi(0) \leqq \psi$ of volume $(\pi^3/6)d^{-1}b^{-2}\psi^3$ is centered on the point $(-R,0,0,0,-R,0)$. Equation (23) gives the probability density at that point and hence the result

$$F(\psi) = \psi^3/\{12N^3db^2 \exp\,(3R^2/2N)\} \tag{25}$$

approximately for small ψ.

APPENDIX D

Correlation coefficients

To prove (10) write,

$$E(\psi_1\psi_2) = 4dDE(\psi_E(0)\psi_E(P)) + 4dBE(\psi_E(0)\psi_H(P))$$
$$+ 4bDE(\psi_H(0)\psi_E(P)) + 4bBE(\psi_H(0)\psi_H(P)). \tag{26}$$

The four expectations on the right are:

$$E\{\psi_E(0)\psi_E(P)\} = N(N-1)\{1 + J_0^2(\beta r)\} + \tfrac{1}{4}NE(|A|^4) \quad (27)$$

$$\begin{aligned} E\{\psi_E(0)\psi_H(P) &= E\{\psi_H(0)\psi_E(P)\} \\ &= N(N-1)\{1 + J_1^2(\beta r)\} + \tfrac{1}{4}NE(|A|^4) \end{aligned} \quad (28)$$

$$\begin{aligned} E\{\psi_H(0)\psi_H(P)\} &= N(N-1)\{1 + \tfrac{1}{2}J_0^2(\beta r) + \tfrac{1}{2}J_2^2(\beta r)\} \\ &\quad + \tfrac{1}{4}NE(|A|^4). \end{aligned} \quad (29)$$

The proofs of (27), (28), (29) are alike. Only $E\{\psi_E(0)\psi_H(P)\}$ will be derived in detail.

Begin with

$$2\psi_E(0) = |\sum_u A(u)|^2$$

$$2\psi_H(P) = |\sum_u A(U)U \exp - i\beta U\cdot P|^2.$$

Then,

$$\psi_E(0)\psi_H(P) = \tfrac{1}{4}\sum_{u,v,U,V} A(u)A^*(v)U\cdot VA(U)A^*(V)\exp i\beta(V-U)\cdot P \quad (30)$$

with the summation variables u,v,U,V ranging over all N^4 ways of picking four vectors from $u_1, \cdots, u_N$. Now take the expectation of both sides of (30). Most of the N^4 terms in the sum have zero expectations because $E(A(u)) = E(A^2(u)) = 0$, and because $A(u)$, $A(v)$ are independent when $u \neq v$. Nonzero expectations can come from terms of three types:

(i) $N(N-1)$ terms with $v = u$, $V = U$, and $U \neq u$,
(ii) $N(N-1)$ terms with $V = u$, $v = U$, and $U \neq u$,
(iii) N terms with $u = v = U = V$.

The expectation of each term of type (i) is

$$\begin{aligned} E(|A(u)|^2U\cdot U\,|\,A(U)|^2) &= \tfrac{1}{4}E(|A(u)|^2)E(|A(U)|^2) \\ &= \tfrac{1}{4} \times 2 \times 2 = 1. \end{aligned}$$

All $N(N-1)$ terms contribute $N(N-1)$ to (28).

The expectation of each term of type (ii) is

$$\tfrac{1}{4}E\{|A(u)|^2|A(U)|^2u\cdot U \exp i\beta(u-U)\cdot P\}$$

$$= E\{u\cdot U \exp i\beta(u-U)\cdot P\}$$

Now let ϑ and Θ be the angles which u and U make with the vector P so that $u \cdot U = \cos(\vartheta - \Theta) = \cos\vartheta \cos\Theta + \sin\vartheta \sin\Theta$ and $(u - U)\cdot) = r\cos\vartheta - r\cos\Theta$. The expectation sought is

$$E\{\cos(\vartheta - \Theta) \exp i\beta r(\cos\vartheta - \cos\Theta)\}$$
$$= \left\{ \left| \int_0^{2\pi} \cos\vartheta \exp(i\beta r\cos\vartheta) d\vartheta/2\pi \right|^2 + \left| \int_0^{2\pi} \sin\vartheta \exp(i\beta r\cos\vartheta) d\vartheta/2\pi \right|^2 \right\}.$$

The two integrals may be recognized as Fourier coefficients in the well-known series

$$\exp(i\beta r\cos\vartheta) = J_0(\beta r) + 2\sum_{n=1}^{\infty} i^n J_n(\beta r)\cos n\vartheta.$$

Then each of $N(N-1)$ terms of type (ii) contributes $J_1^2(\beta r)$ to (28).

Each term of type (iii) is $\frac{1}{4}|A(u)|^4$; the total contribution to (28) of all N terms is $\frac{1}{4}NE(|A|^4)$.

APPENDIX E

Spectra

The normalized power spectrum of $\psi(V_0 t)$ is a Fourier transform of $E(\psi(0)\psi(V_0 t))/E(\psi^2(0))$. The expectations are obtainable from (10) with $D = d$, $B = b$, $P = V_0 t$ and from $E(\psi(0)) = E(\psi(V_0 t)) = 2N$. When N is large, one seeks the transform of

$$\frac{1 - d^2 J_0^2(\beta r) + 2\,db\,J_1^2(\beta r) + \frac{1}{2}b^2(J_0^2(\beta r) + J_2^2(\beta r))}{1 + d^2 + \frac{1}{2}b^2} \tag{31}$$

with $r = |V_0|\,t$.

The constant term in (31) represents the spectral line described in Section VIII. The remaining terms may be transformed using the equation

$$\int_{-\infty}^{\infty} J_n^2(x)\cos xy\,dx = \begin{cases} P_{n-\frac{1}{2}}(\frac{1}{2}y^2 - 1), & 0 < y < 2 \\ 0, & 2 < y < \infty \end{cases}$$

(Ref. 2, Erdelyi, *et al*, p. 46, transform 21), where $P_{n-\frac{1}{2}}(u)$ is the Legendre function of order $n - \frac{1}{2}$.

This result is applied in the form

$$\int_{-\infty}^{\infty} J_n^2(\beta \mid V_0 t \mid) \cos 2\pi f t \, dt = (-1)^n P_{n-\frac{1}{2}}(2\nu^2 - 1)/(\pi f_0)$$

for $0 \leqq \nu \leqq 1$ (recall (14) and $\nu = f/f_0$). One then obtains an expression for $s(f)$ which involves Legendre functions of orders $-\frac{1}{2}$, $\frac{1}{2}$, and $\frac{3}{2}$. This expression was not suitable for computing because there was no available table of Legendre functions of fractional order. However, the Legendre functions of half-integer order can be expressed as complete elliptic integrals by the following identities:

$$P_{-\frac{1}{2}}(x) = (2/\pi)K\{(\tfrac{1}{2} - \tfrac{1}{2}x)^{\frac{1}{2}}\}$$

$$P_{\frac{1}{2}}(x) = (2/\pi)\{2E((\tfrac{1}{2} - \tfrac{1}{2}x)^{\frac{1}{2}}) - K((\tfrac{1}{2} - \tfrac{1}{2}x)^{\frac{1}{2}})\}$$

$$(m+1)P_{m+1}(x) = (2m+1)xP_m(x) - mP_{m-1}(x).$$

(Ref. 1, Abramowitz and Stegun, Eqs. (8.13.1), (8.13.8), (8.13.11)). When the Legendre functions are replaced by elliptic integrals the Bessel function terms of (31) transform into

$$s(f) = \frac{2\{(3 - 4\nu^2 f^2)K((1-\nu^2)^{\frac{1}{2}}) + [(8\nu^2 - 4)b^2 - 12\,db]\,E((1-\nu^2)^{\frac{1}{2}})\}}{3\pi^2 f_0(1 + d^2 + \frac{1}{2}b^2)}. \quad (32)$$

The results (15) and (16) are special cases of (32).

REFERENCES

1. Abramowitz, M., and Stegun, I. A., (editors) *Handbook of Mathematical Functions*, Nat. Bu. Standards, Appl. Math. Series 55, 1964.
2. Erdelyi, A., Magnus, W., Oberhettinger, F., and Tricomi, F. G., *Tables of Integral Transforms, Bateman Manuscript Project*, I, McGraw-Hill, New York, 1954.
3. Ossanna, Jr., J. F., A Model for Mobile Radio Fading Due to Building Reflections: Theoretical and Experimental Fading Waveform Power Spectra, B.S.T.J., *43*, Nov., 1964, pp. 2935–2971.
4. Slack, M., The Probability Distributions of Sinusoidal Oscillations Combined in Random Phase, J.I.E.E., *93*, part III, 1946, pp. 76–86.
5. Young, Jr., W. R., Comparison of Mobile Radio Transmission at 150, 450, 900, and 3700 Mc, B.S.T.J., *31*, 6, 1952, pp. 1068–1085.